Buffer-Gas Loading and Magnetic Trapping of Atomic Europium

Jinha Kim, Bretislav Friedrich, Daniel P. Katz, David Patterson,
Jonathan D. Weinstein, Robert DeCarvalho, and John M. Doyle
Department of Physics, Harvard University, Cambridge, Massachusetts 02138
(Received 13 January 1997)

Atomic europium has been magnetically trapped using buffer-gas loading. Laser ablated Eu($^8S_{7/2}$) atoms are thermalized to 800 mK in a ^{4}He buffer gas (to 250 mK in a ^{3}He buffer gas). Anti-Helmholtz superconducting coils produce a quadrupole magnetic field to trap the $M_J = 7/2$ state of Eu. Detection is via absorption spectroscopy at 462.7 nm. Up to 1×10^{12} Eu atoms are loaded at a central density of 5×10^{12} cm^{-3}. Atoms can be held for longer than 100 s. [S0031-9007(97)03151-7]

PACS numbers: 32.80.Pj, 06.30.Ft, 32.30.Jc, 39.30.+w

Magnetic trapping of atoms has opened up important areas of research including the creation and study of weakly interacting atomic Bose condensates [1], high resolution spectroscopy of atomic hydrogen [2], and the realization of an "atom laser" [3,4]. However, despite the fact that many ground state atoms are paramagnetic (about 70% of the periodic table) [5], only the alkali atoms and atomic hydrogen have been magnetically trapped. This paucity of trapped species is mainly due to the lack of a general technique to load atoms into magnetic traps. Recent efforts in atom trapping have been mostly limited to atomic species whose structure allows for optical cooling; a notable exception is atomic hydrogen which can be cooled by thermalizing with liquid helium films [6,7].

A general technique for loading atomic and molecular species into a magnetic trap was recently proposed by Doyle *et al.* [5]. It is based on the use of a cold helium buffer gas to thermalize the species to energies below the depth of the trap. After thermalization, the helium is (cryo-)pumped away, leaving a thermally isolated, trapped sample. Because buffer-gas loading relies on elastic collisions it is essentially independent of the structure of the trapped species and should therefore find wide application in filling atomic and molecular traps. This feature of the technique is especially important for the case of molecules where the complex energy level structure precludes a simple method for radiative cooling. Trapping is an important step towards ultrahigh resolution spectroscopy of molecules and may find application in improved searches for an elementary particle electric dipole moment [8].

We report magnetic trapping of atomic europium using this buffer-gas loading technique. Eu atoms (vaporized by laser ablation) are thermalized by a He buffer gas and are loaded into a static magnetic trap. Our choice of ground state Eu atoms ($^8S_{7/2}, g = 1.993$) as a test species was led in part by considerations of experimental convenience: The large paramagnetism of Eu makes it easy to trap and the high oscillator strength of its visible transitions makes it easy to detect.

Briefly, our trapping procedure begins with a cryogenic cell filled with either ^{4}He or ^{3}He gas. The cell is inside a spherical quadrupole magnetic trapping field with a depth of up to 2.8 T produced by superconducting coils in an anti-Helmholtz configuration. The cell, and therefore the He gas, is maintained at 800 mK for ^{4}He (250 mK for ^{3}He). Europium atoms are vaporized by laser ablation and thermalized by colliding with the He. Those atoms in low-field seeking states whose kinetic energies are below the trap depth are trapped. After loading, the buffer gas is cryopumped away. The atoms are detected via absorption spectroscopy in the $y^8P_{7/2} - a^8S_{7/2}$ band at 462.7 nm.

The cross-section of the cryogenic apparatus is depicted in Fig. 1. The apparatus consists of four parts: the superconducting magnet, the cryogenic cell, the He can, and the dilution refrigerator. The magnet (5.1 cm diameter clear bore) consists of two NbTi superconducting solenoids encased in a titanium cask. The two coils are oriented in the anti-Helmholtz configuration and therefore repel each other. The repulsive force (of up to 2.5×10^5 N) is taken up by the cask. The individual solenoids are both 2.8 cm thick with an inner and outer diameter of 5.3 and 13.0 cm, respectively. Their centers are separated by 3.3 cm. The entire magnet assembly is immersed in liquid helium.

The cell is positioned at the center of the magnet. It resides in vacuum and is separated from the magnet (and the liquid helium) by a stainless steel vacuum can, a tube of 5 cm diameter and 0.8 mm wall thickness. The cell (inner/outer diameter of 4.27 cm/4.50 cm and length of 6.8 cm) is made of OFE copper with a 4.4 cm diameter fused silica window sealing the bottom. On the inner top surface there is a 1 cm diameter mirror. A solid lump of Eu (the source of the atoms) is positioned near the mirror. The top of the cell is thermally anchored to the mixing chamber of the dilution refrigerator via a copper rod of 1.3 cm diameter. The temperature of the cell can be varied from 100 to 800 mK using a resistive heater.

The purpose of the He can is to allow the helium buffer gas to be cryopumped out of the cell. The He can is connected to the cell through a 3.8 cm diameter thin-walled stainless steel tube. The tube allows gas to flow freely between the cell and the can. The He can is connected to the mixing chamber with a 2 cm diameter copper rod.

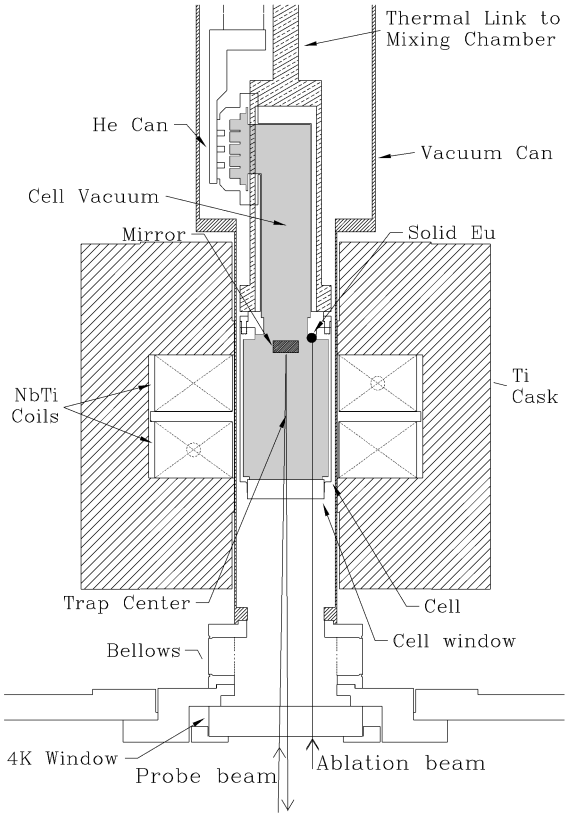

FIG. 1. Schematic diagram of magnetic trapping and optical detection apparatus. The superconducting magnet is immersed in liquid helium. Optical access to room temperature is provided by a set of borosilicate and fused silica windows at the cell temperature, 4, 77, and 300 K. Only the cell and 4 K windows are shown in the figure. The 77 and 300 K windows lie directly below the 4 K window. The YAG beam and the probe beam enter through the same set of windows.

Our detection method is absorption spectroscopy. A probe beam at 462.7 nm is produced using a $KNbO_3$ crystal to double the output of an actively stabilized Ti:sapphire laser (Coherent 899-21). The typical (doubled) power used to probe the atoms is 0.1 μW. The 3.5 ± 1.5 mm diameter beam enters at an angle of about 2° with respect to the cell axis and passes through the cell center with an offset of 3 ± 1.5 mm. The beam then reflects from the mirror at the top of the cell, passes the cell center again, exits the cell, and is detected by a photomultiplier tube.

A pulsed doubled yttrium-aluminum-garnet (YAG) laser beam (Continuum I-10, 532 nm, 5 ns pulse width, 15 mJ typical pulse energy) is used to ablate solid Eu metal (99.9% pure, with the ^{151}Eu and ^{153}Eu isotopes in their natural abundances of 48% and 52%, respectively).

We investigated the thermalization of laser ablated Eu as a function of He temperature, ranging between 300 K and 250 mK. In this preparatory work the Eu atoms were detected by absorption spectroscopy within the (red) $z^{10}P_{7/2} - a^8S_{7/2}$ band (4 μs lifetime, 710.8 nm). The Eu temperature was measured using the Doppler width of the hyperfine lines. With 4 μmol of ^{3}He (loaded into the 95 cm^3 cell), the ablated atoms were found to thermalize with the He gas on a time scale of 1 ms at 77 K, 4 ms at 4 K, and 30 ms at 250 mK. These times are consistent with a simple model of thermalization using a He-Eu elastic collision cross section of 10^{-14} cm^2 at 4 K.

The trap is typically loaded using ^{4}He as buffer gas and with a magnetic trap depth of $B_{\max} = 1.7$ T ($B_{\max} = 0.52$ T with ^{3}He buffer gas). The density of the buffer gas is determined by its vapor pressure and needs to be high enough to thermalize the europium atoms before they impinge on the cell wall (where, presumably, they stick and are lost). The trapping procedure begins by using a heater to raise the cell temperature to 800 mK (250 mK with ^{3}He). A single YAG pulse ablates the lump of europium and the heater is simultaneously turned off. The temperature of the cell rises for about 1 s due to heating by the YAG pulse but then quickly decreases. Over the course of 20 s the temperature of the cell and the He can drops to 230 mK (170 mK with ^{3}He) where the ^{4}He density is about 1×10^4 cm^{-3} (4×10^{13} cm^{-3} with ^{3}He) [9,10]. These densities correspond to room temperature pressures of 3×10^{-13} Torr (1.3×10^{-3} Torr for ^{3}He). The trapped atoms are then probed with the blue beam tuned to the $y^8P_{7/2} - a^8S_{7/2}$ band (6 ns lifetime, 462.7 nm) [11].

Data are taken in one of two ways: Either absorption time profiles at given wavelengths are measured or the laser is scanned over the entire absorption band of about 13 GHz at certain fixed delay times after the ablation pulse. The absorption spectrum can be measured many times for each trapped sample, yielding good signal to background ratios.

Figure 2 shows sample spectra of the trapped ensemble at 0.52 T trap depth (250 mK loading temperature) measured 20, 40, and 60 s after the ablation pulse. One can see that the main features of the spectra change little with time but their integrated absorption intensities are proportionately decreasing.

The experimental spectra were compared to theoretical simulations (described below). These comparisons allowed the determination of total atom number, density and temperature. The trap spectra were assigned on the basis of the spectral constants of ^{151,153}Eu taken from Ref. [12] and the distribution function of the number of atoms subject to a given B field, $N(B)$. The latter was determined for a given magnetic state and loading temperature from the calculated spatial distribution of the B field and factors accounting for the probe beam geometry.

At $B = 0$, the hyperfine populations are determined essentially by the degeneracy factors, $P(F) \rightarrow (2F + 1)$, i.e., all states $|F, M\rangle$ have the same weight. This was corroborated by our measurements. The intensities $\mathcal{I}$ of the transitions between states in absorption spectra are then given by $\mathcal{I} = PS$ where S is the line strength. The spectra of the trapped atoms are simulated by summing up computed spectra pertaining to all field strengths (B) and weighting each by the corresponding factor $N(B)$. Thus,

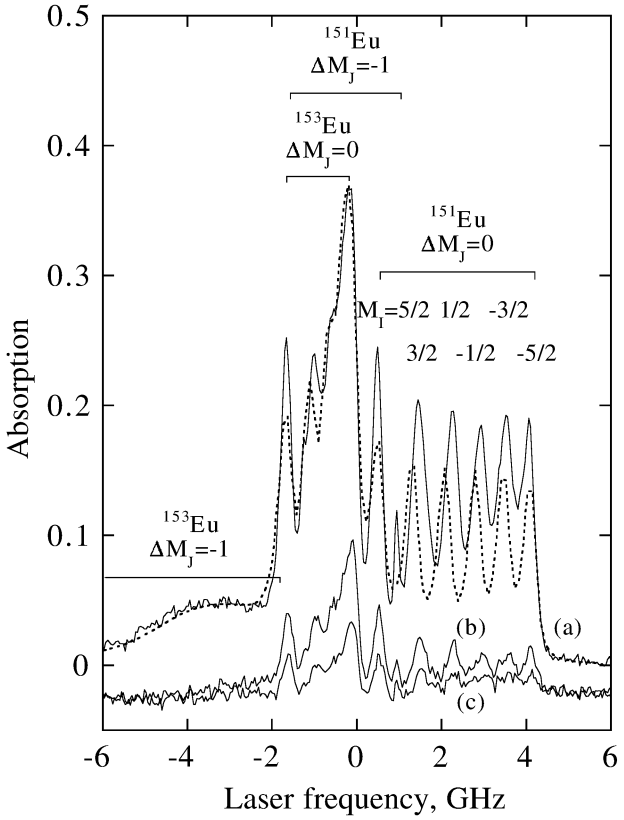

FIG. 2. Sample absorption spectra of the trapped ensemble of Eu in a 0.6 T deep trap at 462.7 nm ($y^8P_{7/2} - a^8S_{7/2}$ band) measured (a) 20 s, (b) 40 s, and (c) 60 s after the ablation pulse. For clarity, the (b) and (c) spectra are shifted on the absorption scale by –0.025. The simulated spectrum, shown by the dotted line, provides the indicated assignment of the lines: All features are due to the $M_J = 7/2$ state of Eu($^8S_{7/2}$). For each isotope, there are two subbands of magnetic hyperfine transitions, with $\Delta M_J = 0$ and -1. Note that for the $\Delta M_J = 0$ transitions in ^{151}Eu, all six M_I nuclear spin states are clearly resolved.

the spectrum is determined by temperature, beam geometry, and the identity of the states trapped. Moreover, at $B_{\max} = 0.52$ T, more than 90% of the detected trapped atoms are subject to $B > 0.05$ T where the strong-field limit is reached (the Paschen-Back hyperfine uncoupling). As a result, the trap spectrum can be simulated analytically, with eigenenergies

$$E(M_J, M_I) = M_J g_J \mu_B B + M_I g_I \mu_B B + a M_J M_I + \frac{9b}{4I(2I-1)J(2J-1)} \times \left[M_J^2 - \frac{1}{3} J(J+1) \right] \times \left[M_I^2 - \frac{1}{3} I(I+1) \right], \quad (1)$$

where J and I are the electronic and nuclear angular momentum quantum numbers ($J = 7/2$ for both electronic states, $I = 5/2$ for both isotopes), M_J and M_I are their projections on the space fixed axis, g_J and g_I are the corresponding g-factors, a and b are the hyperfine magnetic dipole and electric quadrupole coupling constants, and μ_B is the Bohr magneton [13]. The corresponding line strength factors $S_q(M_J', M_I'; M_J, M_I)$ of electric dipole transitions between states $|M_J', M_I'\rangle \leftarrow |M_J, M_I\rangle$ are

$$S_q \propto \delta(M_I', M_I) \langle J, M_J, J', M_J'; 1, q \rangle^2 \quad (2)$$

with $q = 0$ for parallel and $q = \pm 1$ for perpendicular transitions.

From the simulations it follows that essentially only the $M_J = 7/2$ state is trapped. This corresponds well with our model of loading: The lower M_J states are not as tightly confined and leave the trap quickly. The corresponding simulated spectrum together with the assignment of the lines according to the isotope and hyperfine substate is also shown in Fig. 2. With this assignment, the initial temperature of the atoms in ^{3}He could be determined to be 250 ± 50 mK.

We also measured the absorption time profiles at fixed laser frequency and used the data to study the loss kinetics of the atoms from the trap. The absolute atom number was determined using the fitted values from the simulation of the spectra and the published line strength factors [14]. The atomic densities are a natural product of the same calculations. Our atom density and number is determined within ±60%. Figure 3 shows the time profile for ^{4}He and ^{3}He loading (upper and lower panel, respectively), assuming the atoms remain at the initial loading temperature. An initial density of 5×10^{12} cm^{-3} with an initial atom number of 1×10^{12} was achieved with ^{3}He loading.

The ^{4}He data (from 0 to 120 s) fit poorly to an exponential function (one-body loss). A combined Eu-Eu two-body loss and one-body loss yields good fits. This combined fit is dominated by two-body loss and is shown as the smooth dashed line in the figure. Using only the data after the ^{4}He is pumped out (20–120 s) yields similar quality fits for either two-body or one-body loss. These fits result in an effective two-body collisional loss rate constant of $3 \pm 2 \times 10^{-13}$ cm^3 s^{-1} or an exponential time constant of 70 ± 10 s. However, after cryopumping ($t > 20$s) the trapped sample is out of thermal contact with the cell walls and the temperature of the sample may change due to evaporative cooling. This uncertainty prevents rigorous interpretation of these loss rates.

The ^{3}He data also fit poorly assuming only a constant one-body loss but do fit well to two-body $(1/t)$ loss. A combined one-body and two-body loss function was fit to the data. From this and fits of similar data we determined the loss to be two-body with an effective two-body collisional loss rate constant of $2.5 \pm 1.5 \times 10^{-13}$ cm^3 s^{-1} at a temperature of 170 mK. Unlike the ^{4}He case, here the sample is in thermal contact with the cell wall. Fits performed assuming a three-body process (Eu-Eu-Eu) yielded similar quality fits to the two-body

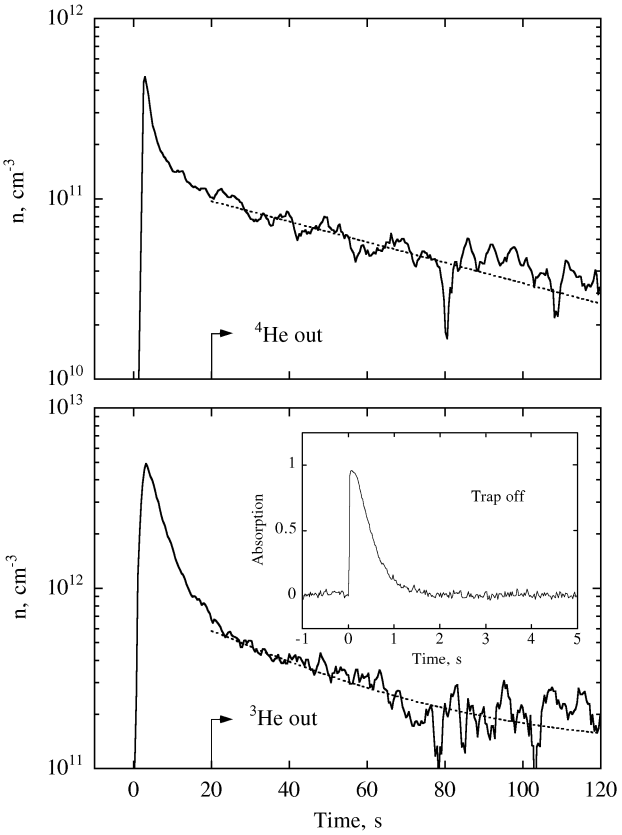

FIG. 3. Averaged absorption time profiles (full line) for ^{4}He (top) and ^{3}He (bottom) loading at 800 mK with ^{4}He (250 mK with ^{3}He) measured at a fixed frequency of the laser (close to the band origin). 4 (8) time profiles were averaged to obtain the displayed ^{4}He (^{3}He) data. Note that about 20 s after the ablation pulse (time zero) the density of the buffer gas drops to about 5×10^4 cm^{-3} (4×10^{13} cm^{-3} for ^{3}He). The data are fitted with a combined one-body and two-body loss rate function (dashed line). About 1×10^{12} atoms are initially loaded into the trap using ^{3}He as a buffer gas. It was experimentally determined that optical pumping was negligible at the probe power levels used. The inset on the right shows an absorption time profile measured under the same conditions, but with the trap off.

fits. Thus, three-body loss cannot be ruled out, although it seems unlikely given the Eu densities present in the trap.

In summary, we have trapped atomic europium using the buffer-gas loading technique. Either ^{4}He or ^{3}He was used as buffer gas. Samples of trapped Eu were held for longer than 100 s. Loss from the trap was observed and studied. Under the assumption that the loss is due to Eu-Eu collisions, the effective two-body loss rate constant is $(2.5 \pm 1.5) \times 10^{-13}$ cm^3 s^{-1} at 170 mK. Given the high initial densities present, it is likely that evaporative cooling can be used to cool the trapped species. Similar to evaporative cooling, buffer-gas loading is based on elastic scattering and therefore is effective independent of many of the details of internal level structure. We believe that this technique can be extended to all paramagnetic atoms and molecules, as well as to other trap types (e.g., light traps). In addition, high magnetic moment atomic species ($\geq 5\mu_b$) should be trappable using a simpler, pumped-liquid-^{4}He refrigerator to cool the buffer gas [5].

This material is based upon work supported by the National Science Foundation under Grant No. PHY-9511951. One of us (J. D. W.) is supported by a National Science Foundation Graduate Research Fellowship.

[1] M. H. Anderson *et al.,* Science **269**, 198 (1995); K. B. Davis *et al.,* Phys. Rev. Lett. **76**, 3969 (1995); C. C. Bradley *et al.,* Phys. Rev. Lett. **78**, 985 (1997).
[2] C. L. Cesar *et al.,* Phys. Rev. Lett. **77**, 255 (1996).
[3] M.-O. Mewes *et al.,* Phys. Rev. Lett. **78**, 582 (1997).
[4] M. R. Andrews *et al.,* Science **275**, 637 (1997).
[5] J. M. Doyle, B. Friedrich, J. Kim, and D. Patterson, Phys. Rev. A **52**, R2515 (1995).
[6] See special issue on Laser Cooling and Trapping of Atoms [J. Opt. Soc. Am. B **6**, 2020 (1989)]; *Proceedings of the Thirteenth-International Conference on Atomic Physics, Munich, 1992* (AIP, New York, 1993); *Fundamental Systems in Quantum Optics 1990*, Proceedings of the Les Houches Summer School (North-Holland, Amsterdam, 1992).
[7] N. Masuhara *et al.,* Phys. Rev. Lett. **61**, 935 (1988).
[8] E. A. Hinds and K. Sangster, in *Time Reversdal—The Arthur Rich Memorial Symposium,* edited by M. Skalsey, P. H. Bucksbaum, R. S. Conti, and D. W. Gidley, AIP Conf. Proc. No. 270 (AIP, New York, 1993), p. 77.
[9] J. Wilks, in *The Properties of Liquid and Solid Helium* (Clarendon Press, Oxford, 1987), vapor pressure of ^{4}He is determined from extrapolation of data present in this reference.
[10] J. Res. Natl. Bur. Stand. A **68**, 579 (1964), densities of ^{3}He gas are determined from extrapolation of data present in this reference.
[11] K. B. Blagoev and V. A. Komarovskii, At. Data Nucl. Data Tables **56**, 1 (1994).
[12] G. J. Zaal *et al.,* Z. Phys. A **290**, 339 (1979).
[13] N. F. Ramsey, in *Molecular Beams* (Oxford University Press, London, 1955).
[14] C. H. Corliss, *Experimental Transition Probabilities for Spectral Lines of Seventy Elements* (U.S. Department of Commerce, NBS, Washington, DC, 1962).